

**In-medium  $\Lambda$  isospin impurity from charge symmetry breaking in the  ${}^4_\Lambda\text{H}$ - ${}^4_\Lambda\text{He}$  mirror hypernuclei**

M. Schäfer, N. Barnea, and A. Gal

*Racah Institute of Physics, The Hebrew University, Jerusalem 91904, Israel*


(Received 22 February 2022; revised 15 April 2022; accepted 19 August 2022; published 20 September 2022; corrected 16 March 2023)

The  $\Lambda$  separation energies in the mirror hypernuclei  ${}^4_\Lambda\text{H}$ - ${}^4_\Lambda\text{He}$  exhibit large charge symmetry breaking (CSB). Analyzing this CSB within pionless effective field theory while using partially conserved baryon-baryon SU(3) flavor symmetry, we deduce a  $\Lambda$ - $\Sigma^0$  induced in-medium admixture amplitude  $\mathcal{A}_{I=1} \approx 1.5\%$  in the dominantly isospin  $I = 0$   $\Lambda$  hyperon. Our results confirm the free-space value  $\mathcal{A}_{I=1}^{(0)}$  inferred directly within the SU(3) baryon octet by Dalitz and von Hippel in 1964 and reaffirmed in a recent QCD+QED lattice calculation. Furthermore, exploring the consequences of SU(3) flavor symmetry on the  $\Lambda$ -nucleon interaction, we find that CSB is expected to impact the  $S = 1$  and  $S = 0$  spin channels in opposite directions, with the latter dominating by an order of magnitude. These observations explain a recent deduction of  $\Lambda$ -nucleon CSB strengths.

 DOI: [10.1103/PhysRevC.106.L031001](https://doi.org/10.1103/PhysRevC.106.L031001)

**Introduction.** Renormalization of hadron decay constants in nuclear matter is a recurring theme in hadronic physics. Well known examples are the roughly 30% in-medium quenching of the pion decay constant  $f_\pi$  and the weak-decay axial-vector constant  $g_A$ . The quenching of  $f_\pi$  was inferred from deeply bound  $\pi^-$ -atom levels in heavy nuclei [1], soon shown by Friedman to hold over the whole periodic table [2], in line with a chiral-symmetry partial restoration argument by Weise [3]. The quenching of  $g_A$  was noticed by Wilkinson in nuclear Gamow-Teller  $\beta$  decays [4] and soon attributed by Rho [5] to spin-isospin correlations manifest in the Ericson-Ericson-Lorentz-Lorenz renormalization of the  $p$ -wave pion-nucleus optical potential [6].

Less explored is the  $S = -1$  strange hadronic sector, where the poorer database of  $\Lambda$  hypernuclei [7] limits the deduction of in-medium trends. A particularly interesting question is whether and how far the Dalitz-von Hippel (DvH) [8] relatively large amplitude  $\mathcal{A}_{I=1}^{(0)} \approx 1.5\%$  of an  $I = 1$  admixture in the dominantly  $I = 0$   $\Lambda$  hyperon gets renormalized in dense matter.  $\mathcal{A}_{I=1}^{(0)}$  was inferred by DvH from the  $\Lambda$ - $\Sigma^0$  mass-mixing matrix element  $M_{\Sigma^0\Lambda}$  related in SU(3)-flavor [SU(3)<sub>f</sub>] symmetry to octet baryon electromagnetic mass differences  $\delta M_{BB'} = M_B - M_{B'}$ :

$$M_{\Sigma^0\Lambda} = \frac{1}{\sqrt{3}}(\delta M_{\Sigma^0\Sigma^+} - \delta M_{np}) = 1.14 \pm 0.05 \text{ MeV}, \quad (1)$$

leading to the free-space value

$$\mathcal{A}_{I=1}^{(0)} = M_{\Sigma^0\Lambda} / \delta M_{\Lambda\Sigma^0} = -0.0148 \pm 0.0006. \quad (2)$$

We note that this result holds also in quark models, where SU(3) octet and decuplet baryons are assigned to the **56** SU(6) multiplet, by assuming only one-quark mass terms and two-quark interaction terms [9] but no three-quark interaction terms. More recently, Eq. (2) was confirmed in a QCD+QED lattice calculation [10], although with considerably larger uncertainty of order 30%.

Appreciable  $\Lambda N$  charge symmetry breaking (CSB) is implied by this isospin impurity of the  $\Lambda$  hyperon. Unfortunately, the poorly known two-body  $\Lambda N$  scattering data are limited to  $\Lambda p$ . In  $\Lambda$  hypernuclei [7], CSB affects mirror states ( $N \leftrightarrow Z$ ), e.g., the  $0^+_{\text{g.s.}}$  and  $1^+_{\text{exc.}}$   ${}^4_\Lambda\text{H}$ - ${}^4_\Lambda\text{He}$  levels where differences of  $\Lambda$  separation energies  $B_\Lambda(J^\pi)$  are nonzero:  $\Delta B_\Lambda(0^+_{\text{g.s.}}) = 233 \pm 92 \text{ keV}$  and  $\Delta B_\Lambda(1^+_{\text{exc.}}) = -83 \pm 94 \text{ keV}$ ; see Fig. 1. A particularly precise measure of CSB is given by their difference,  $\Delta\Delta B_\Lambda = 316 \pm 20 \text{ keV}$ , equal to the difference  $\Delta E_\gamma$  between the two  $\gamma$ -ray energies marked red in the figure. This value is about four times larger than the nuclear CSB splitting  $\Delta B_{\text{CSB}}({}^3\text{H}-{}^3\text{He}) = 67 \pm 9 \text{ keV}$  in the mirror core nuclei  ${}^3\text{H}$ - ${}^3\text{He}$  [14]. The  $A = 4$  hypernuclear CSB  $B_\Lambda$  splittings have been studied recently within chiral effective field theory ( $\chi$ EFT) at leading order

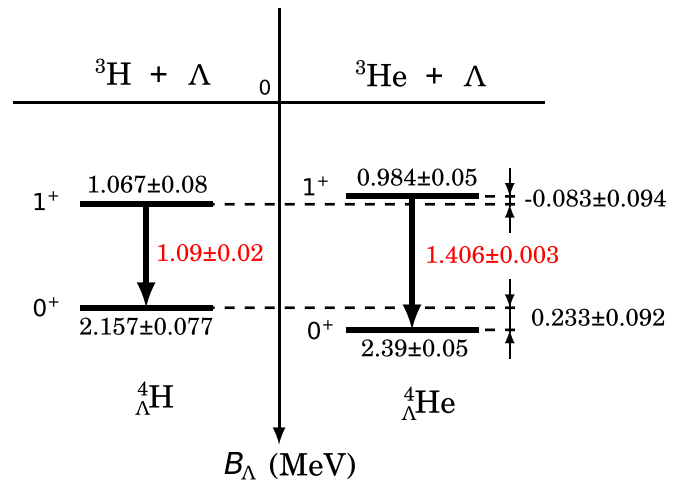


FIG. 1.  $A = 4$  hypernuclear level scheme [11–13] with  $\gamma$ -ray energies [11] marked in red. CSB splittings are shown in MeV to the right of the  ${}^4_\Lambda\text{He}$  levels. Figure adapted from Ref. [13].

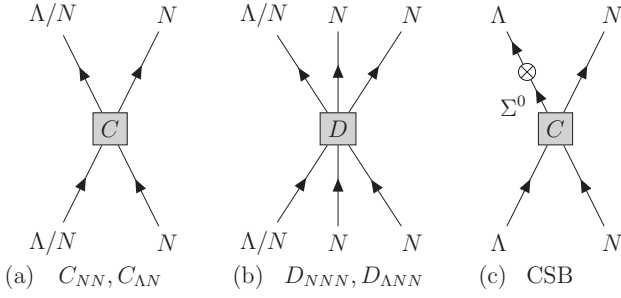


FIG. 2.  $\Lambda$  hypernuclear CS two-body (a) and three-body (b) contact-term diagrams and their associated low-energy constants  $C$  and  $D$ , respectively, plus in (c) a  $\Lambda N \rightarrow \Sigma^0 N$  contact-term diagram, followed by a cross for  $\Lambda$ - $\Sigma^0$  mixing, to illustrate a  $\not{\pi}$ EFT(LO) realization of the CSB ansatz (3).

(LO) [15] and next-to-leading order (NLO) [16]. In the latter work, the  ${}^4_{\Lambda}\text{H}$ - ${}^4_{\Lambda}\text{He}$  splittings were used to estimate the impact of CSB on the  $\Lambda N$  interaction. It was found that CSB acts predominantly on the spin  $S = 0$  channel and that it affects the  $S = 1$  and  $S = 0$  channels in opposite directions, but no satisfactory theoretical argument was given to motivate this difference. Below, we show that these findings are consequences of  $\text{SU}(3)_f$ .

It was noted by DvH that  $\Lambda$ - $\Sigma^0$  mixing induces a long-range, one-pion exchange (OPE), CSB  $\Lambda N$  potential. This result was generalized in Ref. [17] relating the CSB  $\Lambda N$  potential to the charge-symmetric (CS)  $\Lambda N \leftrightarrow \Sigma N$  transition potential,

$$\langle \Lambda N | V_{\text{CSB}} | \Lambda N \rangle = -\frac{2}{\sqrt{3}} \mathcal{A}_{I=1}^{(0)} \langle \Sigma N | V_{\text{CS}} | \Lambda N \rangle \tau_{Nz}. \quad (3)$$

A schematic illustration of this CSB ansatz is given in Fig. 2, diagram (c). The factor 2 emerges from applying  $\Lambda - \Sigma^0$  mixing to either incoming or outgoing  $\Lambda$  states. Projecting the  $I_{YN} = 1/2 \Sigma N$  state on the right-hand side onto its  $\Sigma^0 N$  component produces the factor  $-\tau_{Nz}/\sqrt{3}$ , with  $\tau_{Nz} = \pm 1$  for  $p, n$  respectively.

Here we explore whether the CSB ansatz (3) is satisfied in the  ${}^4_{\Lambda}\text{H}$ - ${}^4_{\Lambda}\text{He}$  mirror hypernuclei, i.e., to what extent the value of  $\mathcal{A}_{I=1}^{(0)}$  is renormalized in matter. To this end we introduce CSB into pionless effective field theory ( $\not{\pi}$ EFT) studies of few-body hypernuclei at LO [18,19]. Since  $\Lambda N$  one-pion exchange (OPE) is forbidden for the dominantly  $I = 0$   $\Lambda$  hyperon, a  $\not{\pi}$ EFT breakup scale  $2m_{\pi}$  is assumed, remarkably close to the threshold value  $p_{\Lambda N}^{\text{th}} \approx 283 \text{ MeV}/c$  for exciting a  $\Sigma N$  pair. Although  $\Sigma$  hyperon degrees of freedom are generally excluded at LO, they may be entered implicitly for  $p_{\Lambda N} \ll 2m_{\pi}$  through a CS  $\Lambda N \leftrightarrow \Sigma N$  transition contact term, such as in Eq. (3), which we relate within a partially conserved  $\text{SU}(3)_f$  to CS  $NN$  and  $\Lambda N$  diagonal contact terms. Doing so, we find that the free-space value  $\mathcal{A}_{I=1}^{(0)} \approx -0.015$  persists also in the  ${}^4_{\Lambda}\text{H}$ - ${}^4_{\Lambda}\text{He}$  mirror hypernuclei.

**Model.** The LO  $\not{\pi}$ EFT interaction for nucleons and  $\Lambda$  hyperons consists of two-baryon  $BB$  and three-baryon  $BBB$   $s$ -wave contact terms shown schematically in Figs. 2(a) and 2(b). These contact terms are given by CS potentials of the

form

$$V_{B_1 B_2}^S = C_{B_1 B_2}^S(\lambda) \mathcal{P}_S \delta_{\lambda}(\mathbf{r}_{12}), \quad (4)$$

and

$$V_{B_1 B_2 B_3}^{IS} = D_{B_1 B_2 B_3}^{IS}(\lambda) \mathcal{Q}_{IS} \sum_{\text{cyc}} \delta_{\lambda}(\mathbf{r}_{12}) \delta_{\lambda}(\mathbf{r}_{23}). \quad (5)$$

Here, the  $\lambda$  ( $\text{fm}^{-1}$ ) dependence attached to the low energy constants (LECs)  $C_{B_1 B_2}^S$  and  $D_{B_1 B_2 B_3}^{IS}$  stands for momentum cutoff values, introduced in a Gaussian form to regularize the zero-range contact terms:

$$\delta_{\lambda}(\mathbf{r}) = \left( \frac{\lambda}{2\sqrt{\pi}} \right)^3 \exp\left(-\frac{\lambda^2}{4} \mathbf{r}^2\right), \quad (6)$$

thereby smearing a zero-range (in the limit  $\lambda \rightarrow \infty$ ) Dirac  $\delta^{(3)}(\mathbf{r})$  contact term over distances  $\sim \lambda^{-1}$ . The cutoff parameter  $\lambda$  may be viewed as a scale parameter with respect to typical values of momenta  $Q$ . To make observables cutoff independent, LECs must be properly renormalized. Truncating  $\not{\pi}$ EFT at LO and using values of  $\lambda$  higher than the breakup scale  $2m_{\pi}$ , observables acquire a residual dependence  $O(Q/\lambda)$  which diminishes with increasing  $\lambda$ . Finally, following the coupled-channel study of Ref. [20], we estimate that excluding explicit  $\Sigma$  hyperon degrees of freedom incurs a few percent error.

In Eq. (4),  $\mathcal{P}_S$  projects on  $s$ -wave  $B_1 B_2$  pairs ( $NN$  or  $\Lambda N$ ) with spin  $S$  associated, for a given cutoff  $\lambda$ , with four two-body LECs  $C_{B_1 B_2}^S$  fitted to low-energy two-body observables, e.g., to the corresponding CS  $NN$  and  $\Lambda N$  scattering lengths. Similarly, in Eq. (5),  $\mathcal{Q}_{IS}$  project on  $NNN$  or  $\Lambda NN$   $s$ -wave triplets with isospin  $I$  and spin  $S$  associated with four three-body LECs  $D_{B_1 B_2 B_3}^{IS}$  fitted to given CS averages of binding energies:  $A = 3$  without  $\Lambda$ ,  $A = 3, 4$  with  $\Lambda$ , thereby making the procedure applied in Ref. [18] explicitly CS. To calculate these binding energies, the  $A$ -body Schrödinger equation is solved variationally by expanding the wave function  $\Psi$  in a correlated Gaussian basis within a stochastic variational method [21]. Convergence to a level of below 1 keV was verified by increasing the number of basis states. The predictive power of CS  $\not{\pi}$ EFT(LO) in the  $s$  shell was already tested in Ref. [18] by calculating binding energies of  ${}^4\text{He}$  and  ${}^5_{\Lambda}\text{He}$  and may soon be tested by comparing the calculated binding energy of  ${}^5_{\Lambda\Lambda}\text{H}$ - ${}^5_{\Lambda\Lambda}\text{He}$  [19], constrained by the  ${}^6_{\Lambda\Lambda}\text{He}$  binding energy datum, with a forthcoming measurement at J-PARC. A  $\not{\pi}$ EFT(LO) approach has been used recently in discussions of the  ${}^3_{\Lambda}\text{H}$  (hypertriton) lifetime [22] and of a likely  $\Lambda nn$  continuum state [23].

Introducing CSB, the two-body  $\Lambda N$  contact terms in  $V_{\Lambda N}$ , Eq. (4), are modified by specifying nucleons as protons or neutrons:

$$C_{\Lambda N}^S \mathcal{P}_S \rightarrow \left( C_{\Lambda p}^S \frac{1 + \tau_{Nz}}{2} + C_{\Lambda n}^S \frac{1 - \tau_{Nz}}{2} \right) \mathcal{P}_S, \quad (7)$$

This suggests to define CS and CSB LECs  $C_{\Lambda N}^S$  and  $\delta C_{\Lambda N}^S$ , respectively, as

$$C_{\Lambda N}^S = \frac{1}{2}(C_{\Lambda p}^S + C_{\Lambda n}^S), \quad \delta C_{\Lambda N}^S = \frac{1}{2}(C_{\Lambda p}^S - C_{\Lambda n}^S). \quad (8)$$

The  $\Lambda N$  interaction assumes then the form

$$V_{\Lambda N} = \sum_S (C_{\Lambda N}^S + \delta C_{\Lambda N}^S \tau_z) \mathcal{P}_S \delta_\lambda(\mathbf{r}_{\Lambda N}). \quad (9)$$

The CSB part of this potential, given in terms of two-body LECs  $\delta C_{\Lambda N}^S$ , is then treated perturbatively with respect to the LO CS wave function. No three-body CSB LECs are necessary at this order. The systematic accuracy of the present CS model calculations is about  $(Q/2m_\pi)^2 \approx 6\%$ , where  $Q \approx \sqrt{2M_\Lambda B_\Lambda} \approx 66$  MeV/ $c$  is a typical momentum scale in  ${}^4\text{H}-{}^4\text{He}$ . The suppression of OPE with respect to the dominant contact-terms contribution found in  $\chi\text{EFT}$  CSB calculations—see, e.g., Ref. [16]—leads to a similar error estimate  $\approx 6\%$  also for the present CSB calculations. Nevertheless, if judged by our residual cutoff dependence, a slightly larger error estimate is suggested. The precise determination of LO error requires consideration of higher order terms.

**Results and discussion.** The  $\Lambda N$  CSB LECs  $\delta C_{\Lambda N}^S$ ,  $S = 0, 1$ , were fitted perturbatively to the two  $A = 4$  binding-energy differences  $\Delta B_\Lambda(0_{\text{g.s.}}^+)$  and  $\Delta B_\Lambda(1_{\text{exc.}}^+)$  shown on the right of Fig. 1. Here we solved the resulting two linear equations for  $\delta C_{\Lambda N}^S$ ,  $S = 0, 1$ , using LO  ${}^4\text{H}(0^+, 1^+)$  wave functions generated by using CS LECs exclusively. Using  ${}^4\text{He}(0^+, 1^+)$  wave functions instead leads to essentially the same result. Readjusting the CS three-body LECs  $D_{\Lambda NN}^S$  within given experimental errors of  $B_\Lambda$ 's in the  $A = 3, 4$  hypernuclear systems incurs only a few percent uncertainties in the fitted CSB LECs. The derived CSB LECs  $\delta C_{\Lambda N}^S$ , of order 1% of the respective  $\Lambda N$  CS LECs  $C_{\Lambda N}^S$ , were used in a distorted-wave Born approximation to produce  $\Lambda N$  scattering length differences  $\delta a_{\Lambda N} = \frac{1}{2}(a_{\Lambda p} - a_{\Lambda n})$ . Since there is no direct experimental extraction of  $\Lambda N$  scattering lengths, we used several model estimates for  $a_S(\Lambda N)$  as input to our calculations. These models, including  $\chi\text{EFT}(\text{LO})$  [26] and  $\chi\text{EFT}(\text{NLO})$  [27] used in recent  $A = 4$  CSB calculations [15,16], respectively, are listed in an inset to Fig. 3 and cited in its caption. The figure shows calculated values of  $2\delta a_S$  as function of the cutoff momentum  $\lambda$  in these  $\Lambda N$  interaction models. In agreement with Ref. [16] we find that CSB hardly affects the spin triplet  $a_{S=1}$ , whereas the singlet  $a_{S=0}$  of order  $\approx (-2.5 \pm 0.5)$  fm is affected strongly, making  $|a_0(\Lambda n)|$  larger by about 0.5 fm than  $|a_0(\Lambda p)|$ , roughly in proportion to  $|a_0|$ . The dominance of  $S = 0$  CSB is shown below to arise naturally from  $\text{SU}(3)_f$  considerations. Interestingly, going to pure neutron matter, the size of the (attractive) spin averaged  $\Lambda N$  scattering length  $(3a_1 + a_0)/4$  increases by only  $\approx 10\%$  from its approximately 2 fm value in symmetric nuclear matter, thereby somewhat aggravating the ‘‘hyperon puzzle’’ [28–30] in neutron star matter.

To check the present extraction of  $a_S(\Lambda p) - a_S(\Lambda n)$  we also applied a similar procedure to the nuclear  $NN$  case. We verified, successfully, that the experimentally derived CSB difference of  $a_0(pp) - a_0(nn) = 1.6 \pm 0.6$  fm in the  $(NN)_{S=0}$  sector can be obtained in  $\not\chi\text{EFT}(\text{LO})$  from the  $A = 3$  nuclear ‘‘datum’’  $\Delta B_{\text{CSB}}({}^3\text{H}-{}^3\text{He}) = 67 \pm 9$  keV [14]. Details will be given elsewhere. Proceeding to the main point of this work, the ansatz Eq. (3), we identify  $\langle \Lambda N | V_{\text{CSB}} | \Lambda N \rangle$  for a given spin value  $S = 0, 1$  with the CSB LEC  $\delta C_{\Lambda N}^S$  extracted directly from the  ${}^4\text{H}-{}^4\text{He}$  spectrum. Similarly, working within the

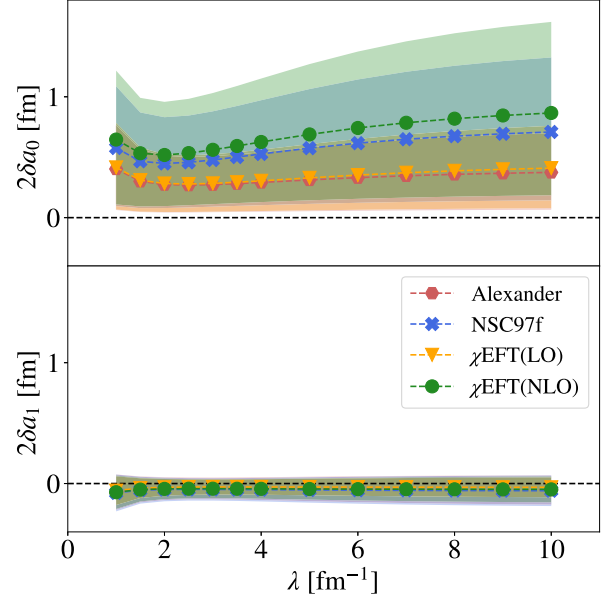


FIG. 3. Scattering length differences  $2\delta a_S = a_S(\Lambda p) - a_S(\Lambda n)$  for  $S = 0$  (upper) and  $S = 1$  (lower) as a function of cutoff momentum  $\lambda$ , derived from  $\delta C_{\Lambda N}^S$  LECs extracted here in  $A = 4$  CSB calculations using  $\Lambda N$  potential models [24–27]; see text. The colored bands represent uncertainties induced by experimental errors in  $\Delta B_\Lambda(0_{\text{g.s.}}^+)$  and  $\Delta B_\Lambda(1_{\text{exc.}}^+)$  values.

framework of  $\not\chi\text{EFT}$ , we identify the spin dependent matrix element  $\langle \Sigma N | V_{\text{CS}} | \Lambda N \rangle$  with a new  $\Sigma N \leftrightarrow \Lambda N$  LEC  $C_{\Sigma N, \Lambda N}^S$ . Following Dover and Feshbach [31], we use  $\text{SU}(3)_f$  to relate  $C_{\Sigma N, \Lambda N}^S$  to the  $NN$  and  $\Lambda N$  CS LECs established in the present application of  $\not\chi\text{EFT}(\text{LO})$ :

$$\begin{aligned} C_{\Sigma N, \Lambda N}^0 &= -3(C_{NN}^0 - C_{\Lambda N}^0), \\ C_{\Sigma N, \Lambda N}^1 &= (C_{NN}^1 - C_{\Lambda N}^1). \end{aligned} \quad (10)$$

In the next step, inspired by Eq. (3), we replace the two CSB LECs  $\delta C_{\Lambda N}^S$  derived from the two binding energy differences  $\Delta B_\Lambda(0_{\text{g.s.}}^+)$  and  $\Delta B_\Lambda(1_{\text{exc.}}^+)$  by two in-medium amplitudes  $\mathcal{A}_{I=1}^S$ ,  $S = 0, 1$ , defined by

$$-\mathcal{A}_{I=1}^S = (\sqrt{3}/2) \delta C_{\Lambda N}^S / C_{\Sigma N, \Lambda N}^S, \quad (11)$$

where the CS LECs  $C_{\Sigma N, \Lambda N}^S$  are expressed through Eq. (10), thereby eliminating any explicit reference to  $\Sigma$  hyperon degrees of freedom. The amplitudes  $\mathcal{A}_{I=1}^S$ ,  $S = 0, 1$ , are shown on the left-hand side of Fig. 4 as function of the cutoff  $\lambda$ , for both  $S = 0$  (upper) and  $S = 1$  (lower) two-body spin states, using the same  $\Lambda N$  interaction models cited in the inset of Fig. 3. These amplitudes exhibit a rather weak dependence on  $\lambda$ , with a common value consistent with (and for  $S = 0$  close to) the DvH value  $-\mathcal{A}_{I=1}^{(0)} = 0.0148$  from Eq. (2).

The results exhibited for  $\mathcal{A}_{I=1}^S$ ,  $S = 0, 1$ , in the left panel of Fig. 4 were derived using the relatively imprecise binding energy differences  $\Delta B_\Lambda(0_{\text{g.s.}}^+) = 233 \pm 92$  keV and  $\Delta B_\Lambda(1_{\text{exc.}}^+) = -83 \pm 94$  keV; see Fig. 1. Using instead the considerably more precise single value  $\Delta E_\gamma = 316 \pm 20$  keV obtained from the difference between the two  $\gamma$  ray energies marked in the figure is, however, insufficient to determine both

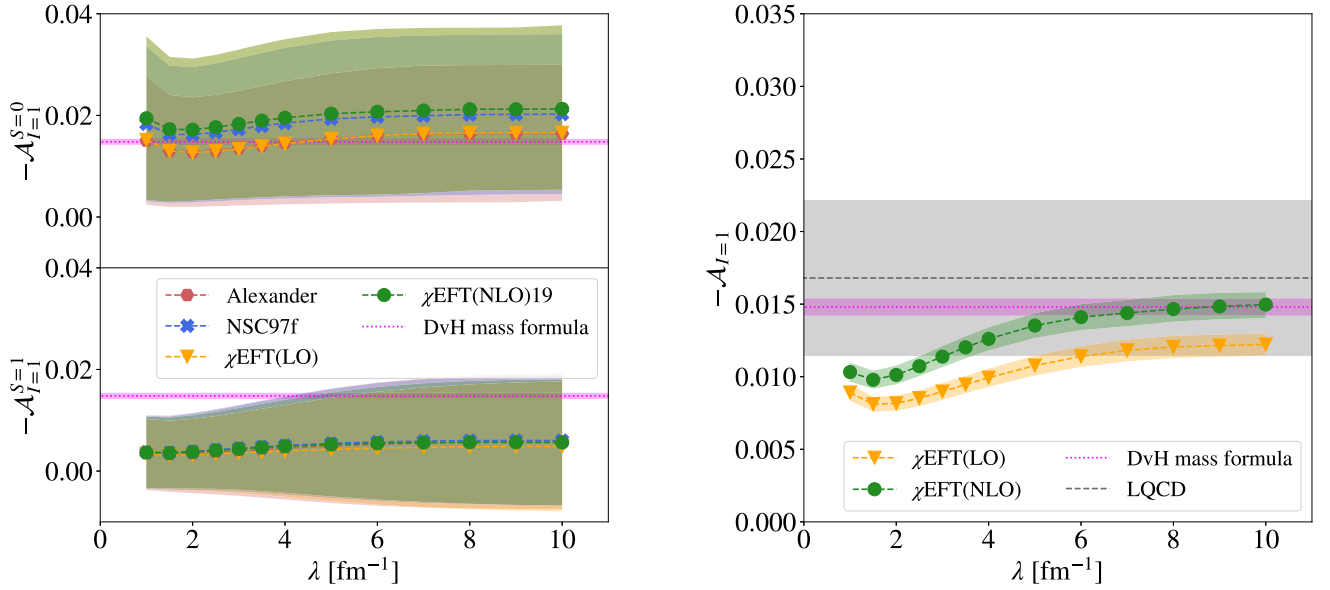


FIG. 4. Left:  $\chi$ EFT estimates for the in-medium DvH amplitudes  $-\mathcal{A}_{I=1}^S = (\sqrt{3}/2)\delta C_{\Lambda N}^S/C_{\Sigma N, \Lambda N}^S$  ( $S = 0$ , upper;  $S = 1$ , lower), with  $\delta C_{\Lambda N}^S$  derived by fitting  $\Delta B_{\Lambda}(0_{g.s.}^+)$  and  $\Delta B_{\Lambda}(1_{exc.}^+)$ , plotted as a function of the cutoff momentum  $\lambda$  and specified in an inset by the  $\Lambda N$  interaction model [24–27] input. Colored bands provide uncertainties caused by  $\Delta B_{\Lambda}$  input values. Right:  $-\mathcal{A}_{I=1}$  values from  $\Delta E_{\gamma} = E_{\gamma}(^4\text{He}) - E_{\gamma}(^4\text{H})$ ; see text. Colored bands provide uncertainties caused by that of  $\Delta E_{\gamma}$ . The horizontal colored intervals mark, in pink, the DvH [8] value of  $-\mathcal{A}_{I=1}^{(0)} = 0.0148 \pm 0.0006$  from Eq. (2), and in grey the LQCD [10] value  $0.0168 \pm 0.0054$ ; see also Table I. Note the expanded vertical scale on the right with respect to that on the left.

$\mathcal{A}_{I=1}^{S=0}$  and  $\mathcal{A}_{I=1}^{S=1}$ . Assuming spin independence to start with, a precise value  $\mathcal{A}_{I=1}$  is derived from  $\Delta E_{\gamma}$  as shown on the right-hand side of Fig. 4. For all four  $\Lambda N$  potential models considered on the left-hand side, the derived value (shown for the  $\chi$ EFT models) is within the LQCD horizontal band for cutoff  $\lambda \gtrsim 6 \text{ fm}^{-1}$ , while for NSC97f [25] and  $\chi$ EFT(NLO) [27] (and also its 2019 version [32]) the derived values do enter the considerably narrower ( $\pm 4\%$ ) DvH  $SU(3)_f$  horizontal band for  $-\mathcal{A}_{I=1}^{(0)}$ . All in-medium isospin  $I = 1$  admixture amplitudes  $-\mathcal{A}_{I=1}$  calculated for  $\lambda \gg 2m_{\pi}$  exhibit a  $\sim \lambda^{-1}$  dependence, and the corresponding values extrapolated to the renormalization scale-invariance limit  $\lambda \rightarrow \infty$  are listed in Table I.

In view of its success, the above procedure can also be applied in reverse. That is, substituting the DvH value  $\mathcal{A}_{I=1}^{(0)}$

TABLE I. Estimates of the  $I = 1$  admixture amplitude  $-\mathcal{A}_{I=1}$  in the  $\Lambda$  hyperon from (i) baryon-number  $B = 1$  free-space studies of DvH and LQCD [8,10] and (ii) the present  $\chi$ EFT(LO)  $B = 4$   $^4_{\Lambda}\text{H}$ - $^4_{\Lambda}\text{He}$  CSB study, using Eq. (3) and input from  $\Lambda N$   $\chi$ EFT models. The  $B = 4$  values are extrapolations to the renormalization scale-invariance limit  $\lambda \rightarrow \infty$  and their listed uncertainties reflect primarily input data uncertainties.

Method/Input	$B$	$-\mathcal{A}_{I=1}$
$SU(3)_f$ [8]	1	$0.0148 \pm 0.0006$
LQCD [10]	1	$0.0168 \pm 0.0054$
$\chi$ EFT(LO)/ $\chi$ EFT(LO) [26]	4	$0.0139 \pm 0.0013$
$\chi$ EFT(LO)/ $\chi$ EFT(NLO) [27]	4	$0.0168 \pm 0.0014$

from Eq. (2) and the  $SU(3)_f$  relations Eq. (10) in Eq. (11), one extracts the CSB LECs  $\delta C_{\Lambda N}^S$  and evaluates the  $A = 4$  CSB splittings  $\Delta B_{\Lambda}(0_{g.s.}^+)$  and  $\Delta B_{\Lambda}(1_{exc.}^+)$ . Doing so, we find that the  $\Delta B_{\Lambda}$  values marked in Fig. 1 are reproduced within their experimental error. We also find that (i) the resulting LECs  $\delta C_{\Lambda N}^0$ ,  $\delta C_{\Lambda N}^1$  have opposite signs, and (ii)  $|\delta C_{\Lambda N}^0| \gg |\delta C_{\Lambda N}^1|$ , implying that CSB acts predominantly on the spin  $S = 0$  channel.

Our results suggest strongly that the  $\Lambda$ 's  $I = 1$  isospin impurity of magnitude  $\approx 1.5\%$  in free space is upheld in the  $A = 4$   $\Lambda$  mirror hypernuclei. This conclusion appears natural in the context of partial restoration of chiral symmetry in dense matter, since there is no direct link known to us between  $\Lambda$ - $\Sigma^0$  mixing and chiral symmetry breaking; for example, the nonstrange quark-mass difference  $m_d - m_u$  does not enter the  $SU(3)_f$  mass mixing matrix element  $M_{\Sigma^0 \Lambda}$ , Eq. (1).

*Closing remarks.*  $\chi$ EFT(LO) applications to few-body hypernuclei are normally limited to  $N$  and  $\Lambda$  degrees of freedom. To consider hypernuclear CSB, the set of two-body and three-body  $s$ -wave CS LECs shown schematically in (a) and (b) of Fig. 2 was extended, adding two  $S = 0, 1$   $\Lambda N$  CSB LECs which were then fitted to the two experimentally available CSB  $A = 4$   $\Delta B_{\Lambda}$  values. The resulting CS broken values of the  $\Lambda N$  scattering lengths shown in Fig. 3 come out then practically the same as those derived within a more involved  $\chi$ EFT(NLO) approach [16] that includes additional  $\Sigma$  hyperon and pseudoscalar octet meson degrees of freedom.

Apart from suggesting an economical way to evaluate CSB in strange matter, we were able to show that CSB is linked uniquely to the  $I = 1$  isospin impurity  $\mathcal{A}_{I=1}^{(0)}$  of the dominantly  $I = 0$   $\Lambda$  hyperon, provided (i) the ansatz (3) is adopted and (ii)

the  $\langle \Sigma N | V_{\text{CS}} | \Lambda N \rangle$  transition matrix element in (3) is related by  $SU(3)_f$  to the  $\langle NN | V_{\text{CS}} | NN \rangle$  and  $\langle \Lambda N | V_{\text{CS}} | \Lambda N \rangle$  matrix elements, each near its own threshold. Having managed to avoid introducing explicitly  $\Sigma$  hyperon degrees of freedom into the employed  $\chi$ EFT(LO) scheme, we are spared of trying to impose  $SU(3)_f$  symmetry simultaneously on all  $\Lambda N$ ,  $\Sigma N$ , and  $\Lambda N \leftrightarrow \Sigma N$  LECs fitted to low-energy scattering and reaction data, proven impossible at LO in  $\chi$ EFT [26] as discussed recently [32] upon introducing a new  $\chi$ EFT(NLO)19 version. It is worth mentioning that two  $\Sigma N$  channels, specifically  $(I = \frac{3}{2}, J^\pi = 1^+)$  and  $(I = \frac{1}{2}, J^\pi = 0^+)$ , are plagued by “Pauli forbidden” six-quark configurations, say  $uuuuds$  for  $I_z = \frac{3}{2}$  of the former channel [33], providing thereby a specific mechanism beyond the scope of  $SU(3)_f$ .

The usefulness of the CSB approach outlined here for the  $A = 4$  mirror hypernuclei, where precise  $\gamma$  ray data exist,

should be tested in heavier hypernuclei when similarly precise CSB data become available. However, phenomenological arguments regarding  $\Sigma$  hyperon admixtures in  $\Lambda$  hypernuclei [17,34] lead us to believe that CSB splittings of  $1s_\Lambda$  mirror levels decrease quickly with  $A$ , making such tests more difficult but nonetheless challenging.

#### ACKNOWLEDGMENTS

A.G. would like to thank Johann Haidenbauer and Wolfram Weise for instructive discussions on EFT approaches to strange few-body systems. The work of M.S. and N.B. was supported by the Pazy Foundation and by the Israel Science Foundation Grant No. 1086/21. Furthermore, the work of A.G. and N.B. is part of a project funded by the European Union’s Horizon 2020 research and innovation program under Grant Agreement No. 824093.

- 
- [1] P. Kienle and T. Yamazaki, *Phys. Lett. B* **514**, 1 (2001); H. Geissel *et al.*, *Phys. Rev. Lett.* **88**, 122301 (2002).
- [2] E. Friedman, *Phys. Lett. B* **524**, 87 (2002); E. Friedman and A. Gal, *ibid.* **578**, 85 (2004), *Nucl. Phys. A* **928**, 128 (2014); *Phys. Lett. B* **792**, 340 (2019).
- [3] W. Weise, *Acta Phys. Pol. B* **31**, 2715 (2000), *Nucl. Phys. A* **690**, 98 (2001); E. E. Kolomeitsev, N. Kaiser, and W. Weise, *Phys. Rev. Lett.* **90**, 092501 (2003).
- [4] D. H. Wilkinson, *Phys. Rev. C* **7**, 930 (1973).
- [5] M. Rho, *Nucl. Phys. A* **231**, 493 (1974); E. Oset and M. Rho, *Phys. Rev. Lett.* **42**, 47 (1979); I. S. Towner and F. C. Khanna, *ibid.* **42**, 51 (1979).
- [6] M. Ericson and T. E. O. Ericson, *Ann. Phys. (NY)* **36**, 323 (1966).
- [7] A. Gal, E. V. Hungerford, and D. J. Millener, *Rev. Mod. Phys.* **88**, 035004 (2016).
- [8] R. H. Dalitz and F. von Hippel, *Phys. Lett.* **10**, 153 (1964).
- [9] A. Gal and F. Scheck, *Nucl. Phys. B* **2**, 110 (1967).
- [10] Z.R. Kordov, R. Horsley, Y. Nakamura, H. Perl, P. E. L. Rakow, G. Schierholz, H. Stuben, R.D. Young, and J. M. Zanotti, *Phys. Rev. D* **101**, 034517 (2020).
- [11] T. O. Yamamoto *et al.* (J-PARC E13 Collaboration), *Phys. Rev. Lett.* **115**, 222501 (2015).
- [12] A. Esser *et al.* (MAMI A1 Collaboration), *Phys. Rev. Lett.* **114**, 232501 (2015).
- [13] F. Schulz *et al.* (MAMI A1 Collaboration), *Nucl. Phys. A* **954**, 149 (2016).
- [14] R. Machleidt and H. Mütter, *Phys. Rev. C* **63**, 034005 (2001).
- [15] D. Gazda and A. Gal, *Phys. Rev. Lett.* **116**, 122501 (2016); *Nucl. Phys. A* **954**, 161 (2016).
- [16] J. Haidenbauer, U.-G. Meißner, and A. Nogga, *Few-Body Syst.* **62**, 105 (2021).
- [17] A. Gal, *Phys. Lett. B* **744**, 352 (2015).
- [18] L. Contessi, N. Barnea, and A. Gal, *Phys. Rev. Lett.* **121**, 102502 (2018).
- [19] L. Contessi, M. Schäfer, N. Barnea, A. Gal, and J. Mareš, *Phys. Lett. B* **797**, 134893 (2019).
- [20] T. D. Cohen, B. A. Gelman, and U. van Kolck, *Phys. Lett. B* **588**, 57 (2004).
- [21] Y. Suzuki and K. Varga, *Stochastic Variational Approach to Quantum Mechanical Few-Body Problems* (Springer-Verlag, Berlin, 1998).
- [22] F. Hildenbrand and H.-W. Hammer, *Phys. Rev. C* **100**, 034002 (2019).
- [23] M. Schäfer, B. Bazak, N. Barnea, A. Gal, and J. Mareš, *Phys. Rev. C* **105**, 015202 (2022), and earlier works listed therein.
- [24] G. Alexander, U. Karshon, A. Shapira *et al.*, *Phys. Rev.* **173**, 1452 (1968).
- [25] Th.A. Rijken, V. G. J. Stoks, and Y. Yamamoto, *Phys. Rev. C* **59**, 21 (1999).
- [26] H. Polinder, J. Haidenbauer, and U.-G. Meißner, *Nucl. Phys. A* **779**, 244 (2006).
- [27] J. Haidenbauer, S. Petschauer, N. Kaiser, U.-G. Meißner, A. Nogga, and W. Weise, *Nucl. Phys. A* **915**, 24 (2013).
- [28] S. Gandolfi and D. Lonardon, *JPS Conf. Proc.* **17**, 101001 (2017).
- [29] I. Bombaci, *JPS Conf. Proc.* **17**, 101002 (2017).
- [30] L. Tolos and L. Fabbietti, *Prog. Part. Nucl. Phys.* **112**, 103770 (2020).
- [31] C. B. Dover and H. Feshbach, *Ann. Phys. (NY)* **198**, 321 (1990).
- [32] J. Haidenbauer, U.-G. Meißner, and A. Nogga, *Eur. Phys. J. A* **56**, 91 (2020).
- [33] M. Oka, K. Shimizu, and K. Yazaki, *Nucl. Phys. A* **464**, 700 (1987).
- [34] A. Gal and D. J. Millener, *Phys. Lett. B* **725**, 445 (2013).

*Correction:* Missing superscripts in Eqs. (4) and (5) and a missing summation in Eq. (9) have been inserted.